Biophys Rep 2025, 11(X):1–14
https://doi.org/10.52601/bpr.2025.250058 https://cstr.cn/32402.14.bpr.2025.250058
Biophysics Reports

RESEARCH ARTICLE

Neutrophils extracellular traps-related lncRNAs as potential biomarkers in lung adenocarcinoma

Yuanyuan Zhao[1], Yingli Chen[1,2] ✉, Qianzhong Li[1,2]

[1] Inner Mongolia Key Laboratory of Biophysics and Bioinformatics, School of Physical Science and Technology, Inner Mongolia University, Hohhot 010021, China
[2] The State Key Laboratory of Reproductive Regulation and Breeding of Grassland Livestock, Inner Mongolia University, Hohhot 010021, China

Received: 1 October 2025 / Accepted: 22 October 2025

Abstract Lung adenocarcinoma (LUAD) is the most common pathological type of lung cancer. Long non-coding RNAs (lncRNAs) can not only serve as independent biomarkers, but also influence the occurrence and development of LUAD through interactions with other RNAs or regulation by the methylated sites in the promoter region. Evidence indicated that the neutrophil extracellular traps (NETs)-related lncRNAs are closely related to the occurrence and development of LUAD. This study aims to identify novel NETs-related lncRNAs and explore their potential regulatory pathways in LUAD progression. We analyzed the differences in lncRNAs, miRNAs, mRNAs expression and β values of methylation sites between normal and tumor samples. NETs-related lncRNAs were identified by the Pearson correlation analysis of NETs-related genes with differentially expressed lncRNAs. On this basis, lncRNA FAM83A-AS1 was screened by differential analysis, Pearson correlation analysis, K-M analysis, multivariate Cox analysis, and ROC curve, which can be used as an early diagnostic marker for LUAD patients. Based on the interaction relationships between lncRNA-miRNA and miRNA-mRNA, a prognostic competitive endogenous RNAs (ceRNAs) network regulated by the NETs-related lncRNA THRB-IT1 was constructed. Finally, by mapping the differentially methylated sites to the promoter region of NETs-related lncRNAs, we identified the key methylation site cg21907579, which regulates the expression of lncRNA TBX5-AS1. The three identified NETs-related lncRNAs are expected to be potential markers and therapeutic targets of LUAD.

Keywords Lung adenocarcinoma, Neutrophil extracellular traps, Long non-coding RNA, Methylation

INTRODUCTION

Lung cancer has become the most prevalent malignant tumor globally in terms of incidence and mortality. It is broadly classified into four histological subtypes: small cell carcinoma, large cell carcinoma, adenocarcinoma, and squamous cell carcinoma. Among these, lung adenocarcinoma (LUAD) is the most common histological subtype (Wei *et al.* 2023). In general, LUAD patients have entered the advanced stage when diagnosed. At present, some patients of advanced stage can only rely on traditional treatment schemes such as chemotherapy and radiotherapy. However, those who receive immunotherapy or targeted treatment regimens may also encounter issues such as drug resistance and mismatched target genes (Zhou *et al.* 2024). Therefore, achieving early diagnosis and identifying novel biomarkers are crucial for guiding the subsequent treatment of patients with LUAD (Chen *et al.* 2023).

Immune cells, also known as white blood cells, are the fundamental components of the human immune system, which can identify and eliminate harmful

✉ Correspondence: stchenyl@imu.edu.cn (Y. Chen)

substances in the human body, such as foreign invasion of bacteria, viruses, aging cells produced in the body and tumor cells, *etc*. Neutrophils are the most abundant immune cells in the human immune system. Upon inflammatory stimulation, they migrate to the target site and eradicate harmful agents through phagocytosis, degranulation, or by releasing a specialized meshwork. This web-like structure, expelled during programmed neutrophil death, is known as neutrophil extracellular traps (NETs) (Papayannopoulos 2018; Sadeghi *et al.* 2023). Cytokines and chemokines produced by tumor cells in the tumor microenvironment attract the infiltration of various immune cells, including neutrophils, leading to the dysregulation of the NETs release process, further increase inflammation and immune dysfunction (Gun *et al.* 2019; Hidalgo *et al.* 2022). In addition, the massive accumulation of NETs can release various protein factors to promote the growth of primary tumors, induce the proliferation of dormant tumor cells, or help tumor cells escape by recruiting platelets to the surface of tumor cells, while tumor cells captured by NETs can adhere to blood vessels for distant metastasis (Chen *et al.* 2021).

Long non-coding RNAs (lncRNAs) are RNA molecules longer than 200 nucleotides that lack protein-coding capacity (Tan *et al.* 2021). LncRNAs were initially thought to be "noise" produced during transcription, and with the deepening of research, the role of lncRNAs in cells has been gradually revealed (Zhang 2024). LncRNAs can not only play an important role in proliferation, apoptosis, differentiation, and other cell activities, but also participate in a large number of biological processes of human disease occurrence, especially in the occurrence and development of malignant tumors, usually accompanied by abnormal expression of lncRNAs (Liu *et al.* 2024; Qi *et al.* 2021). Research indicated that the expression of lncRNAs may be influenced by NETs, thereby playing a role in the process of tumor metastasis. For example, NETs activate the NF-κB/NLRP3 signaling pathway by stimulating the downregulation of lncRNA MIR503HG expression, inducing epithelial-mesenchymal transformation, and promoting metastasis of non-small cell lung cancer, while MIR503HG overexpression can reverse the tumor-promoting effect of NETs (Wang *et al.* 2022). Additionally, by integrating TCGA datasets with RNA-microarray profiles, researchers constructed a 12 NETs-related lncRNAs prognostic signature for non-small-cell lung cancer through co-expression network analysis, LASSO regression, and Cox modeling. RT-qPCR assays subsequently validated the expression of three high-risk lncRNAs and confirmed their altered levels after NETs stimulation (Fang *et al.* 2021).

By integrating the expression data and methylation data of lncRNAs as well as the clinical data of LUAD patients, we identified three key NETs-related lncRNAs and comprehensively evaluated their potential as effective biomarkers for LUAD. The differentially expressed genes between normal and tumor samples were obtained by differential analysis, and lncRNAs that can be used as early diagnostic markers for LUAD patients were screened through Pearson correlation analysis, K-M analysis, multivariate Cox analysis, and ROC curve. Subsequently, a competing endogenous RNAs (ceRNAs) network was constructed by integrating lncRNA–miRNA and miRNA–mRNA interaction data. Within this network, we evaluated the associations of lncRNAs with both patient prognosis and NETs-related genes, ultimately establishing a NETs-related prognostic ceRNA networks for LUAD. Furthermore, we explored the distribution pattern of promoter methylation in LUAD and the correlation between promoter methylation sites and lncRNAs expression associated with NETs. The flowchart of the study contents is shown in Fig. 1.

RESULTS

FAM83A-AS1, a NETs-related lncRNA, as an early diagnostic biomarker for LUAD patients

Identification of NETs-related lncRNAs

Differential expression analysis of lncRNAs, miRNAs, and mRNAs between normal and tumor samples revealed 2750 lncRNAs, 256 miRNAs, and 4707 mRNAs meeting the criteria $P < 0.05$ and $|\log_2 FC| > 1$. 1305 of 2750 DElncRNAs were upregulated and 1445 DElncRNAs were downregulated (Fig. 2A); 125 of 256 DEmiRNAs were upregulated and 131 DEmiRNAs were downregulated (Fig. 2B); and 2137 of 4707 DEmRNAs were upregulated and 2570 DEmRNAs were downregulated (Fig. 2C). Pearson correlation coefficients between the 2750 DElncRNAs and 290 NETs-related genes were calculated. DElncRNAs with $|R| > 0.3$ and $P < 0.05$ were defined as NETs-related lncRNAs, yielding a total of 1380 NETs-related lncRNAs.

Identification of the diagnostic lncRNA FAM83A-AS1

To obtain lncRNAs that can be used as independent prognostic factors, K-M analysis and multivariate Cox analysis were performed on 2750 DElncRNAs, and the obtained 91 lncRNAs were defined as independent

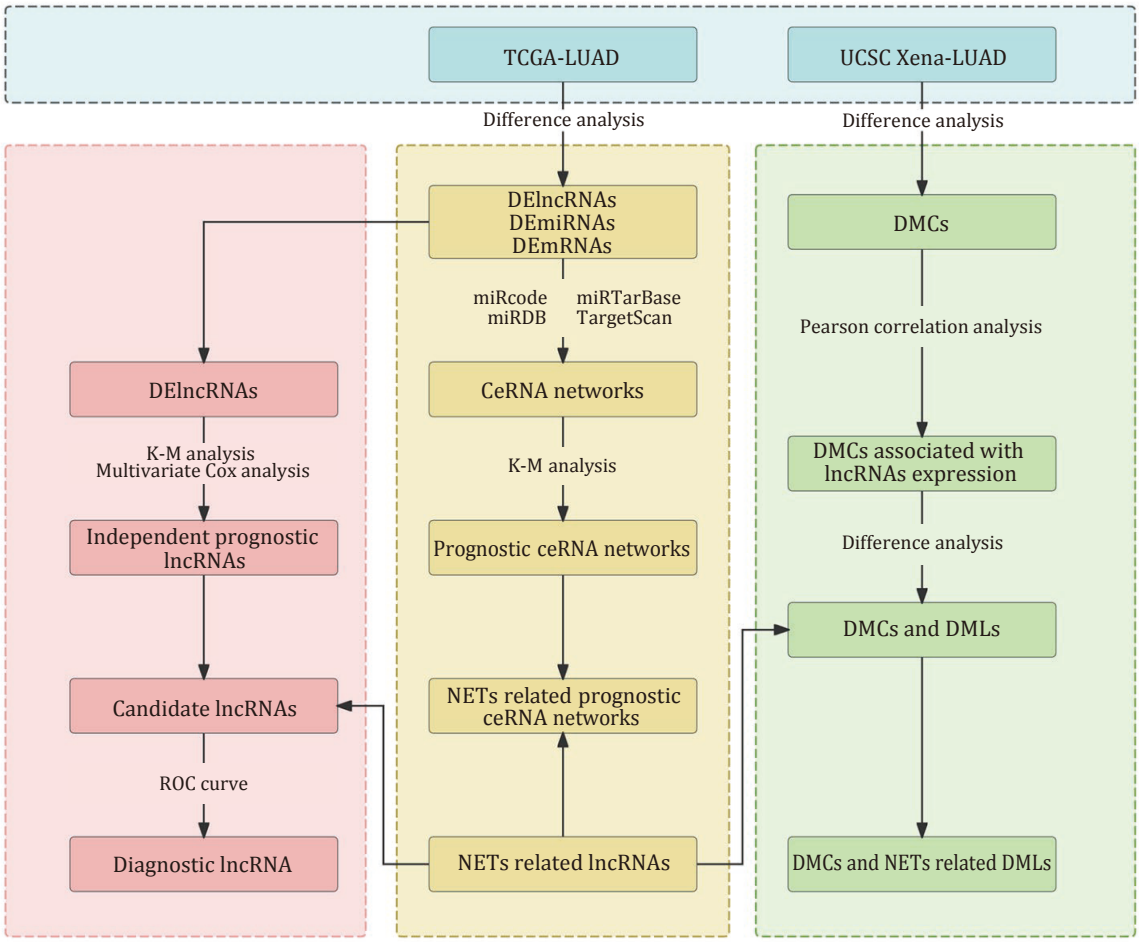

Fig. 1 Flowchart of the work

prognostic lncRNAs. By intersecting 91 independent prognostic lncRNAs with 1380 NETs-related lncRNAs, the overlapping lncRNAs were retained as candidate lncRNAs for early diagnosis of LUAD, yielding a total of 39 candidate lncRNAs. Then, by constructing models of the 39 candidate lncRNAs, we found that the lncRNA FAM83A-AS1 exhibited the highest *AUC,* was identified as the diagnostic lncRNA. Box plots were used to visualize the expression of FAM83A-AS1 between normal and tumor samples. The results revealed the expression differences of FAM83A-AS1 between normal and tumor samples, in which the expression value of FAM83A-AS1 was remarkablely elevated during the progression of LUAD (Fig. 2D). The ROC curve verified the validity of FAM83A-AS1 as a diagnostic lncRNA, and the *AUC* achieves 0.980, indicating that FAM83A-AS1 could better distinguish normal samples from tumor samples in LUAD, and could be used as an ideal diagnostic marker (Fig. 2E).

Prognostic value of the diagnostic lncRNA FAM83A-AS1

Based on FAM83A-AS1 expression, samples were divided into high and low expression groups. The correlations between FAM83A-AS1 expression and OS, PFS, and DSS were investigated by K-M analysis. The K-M curve showed that LUAD patients with the high expression level of FAM83A-AS1 had a lower survival rate and a worse survival situation. Consequently, FAM83A-AS1 expression was negatively correlated with OS, PFS, and DSS (Figs. 3A–3C). The above results indicated that the high expression of FAM83A-AS1 is associated with poor prognosis in LUAD patients. Univariate and multivariate independent prognostic analyses were performed for FAM83A-AS1, age, sex, and pathologic stage. Univariate independent prognostic analysis revealed that FAM83A-AS1 and pathologic stage may serve as independent prognostic factors (Figs. 3D–3F). Multivariate independent prognostic analysis further indicated that, when accounting for

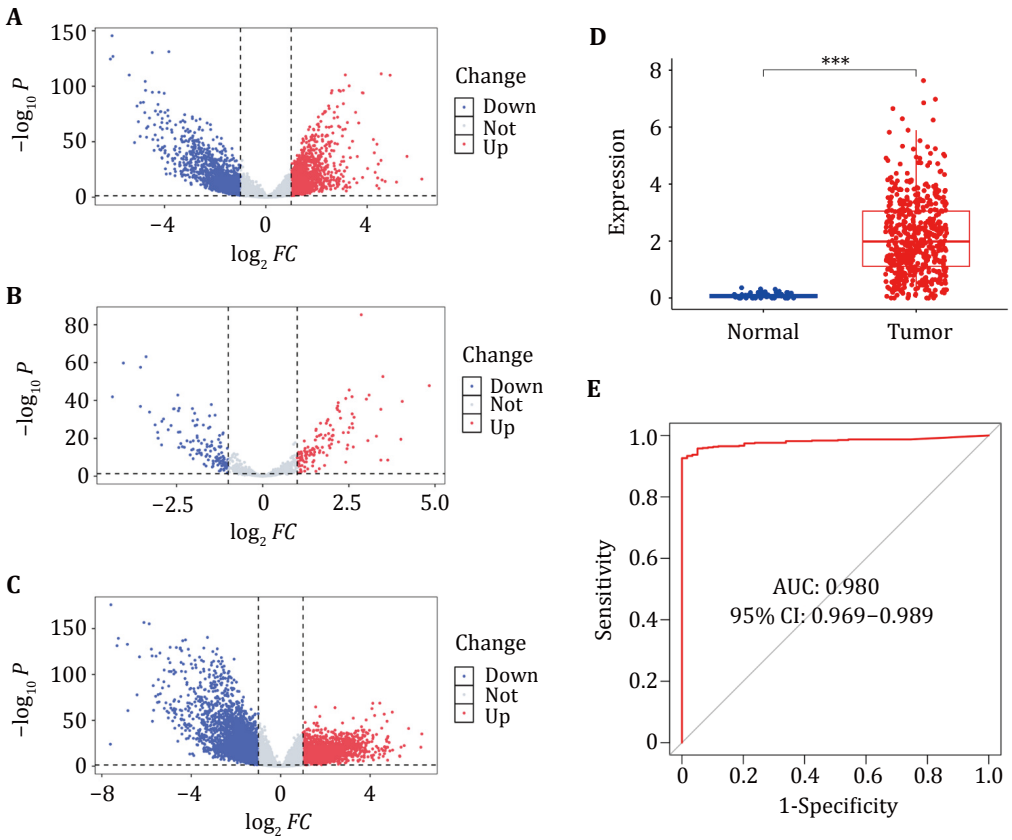

Fig. 2 Screening and identification of FAM83A-AS1. Differentially expressed lncRNAs (**A**), miRNAs (**B**), and mRNAs (**C**) between normal and tumor samples. **D** The expression of FAM83A-AS1 between normal and tumor samples. **E** ROC curve for FAM83A-AS1

interactions among multiple factors, FAM83A-AS1 and pathologic stage remain independent prognostic factors unaffected by other variables, with both acting as protective factors (Figs. 3G–3I). Correlation analysis between FAM83A-AS1 and six clinical characteristics revealed that only pathologic stage and N significantly influence FAM83A-AS1 expression during LUAD development (Fig. 4).

THRB-IT1, a NETs-related lncRNA, regulates prognostic ceRNA networks

Construction of the ceRNA networks

Based on predictions from the miRcode database (http://www.mircode.org/), 150 of the 2750 DElncRNAs formed 714 lncRNA-miRNA interaction pairs with 206 target miRNAs in the database. The intersection of the predicted 206 target miRNAs and the 256 DEmiRNAs yielded 11 DEmiRNAs (Fig. 5A). Next, the target genes of the 11 DEmiRNAs were predicted by using miRDB (http://www.mirdb.org/), miRTarBase (https://mirtarbase.cuhk.edu.cn/), and TargetScan (https://www.targetscan.org/). After retaining only the mRNAs commonly identified by all three databases, we obtained 1003 miRNA–mRNA interaction pairs involving the 11 DEmiRNAs and 860 unique target mRNAs. Similarly, the intersection of the predicted 860 target mRNAs and the 4707 DEmRNAs yielded 166 DEmRNAs (Fig. 5B). Finally, integrating the DElncRNA-DEmiRNA and DEmiRNA-DEmRNA interactions described above, we obtained a ceRNA network, which contained 79 lncRNAs, 9 miRNAs, and 85 mRNAs (Fig. 5C).

Construction of the prognostic ceRNA networks

Based on the median expression levels of 79 lncRNAs within the ceRNA networks, samples were divided into high and low expression groups. K-M analysis was performed on the high and low expression groups, and six lncRNAs (LINC00535, C5orf64, CLDN10-AS1, LINC00518, THRB-IT1, and LNX1-AS2) associated with OS in LUAD patients were obtained. Compared with the survival rate of the low expression group, the survival rate of the high expression group of LINC00535 and

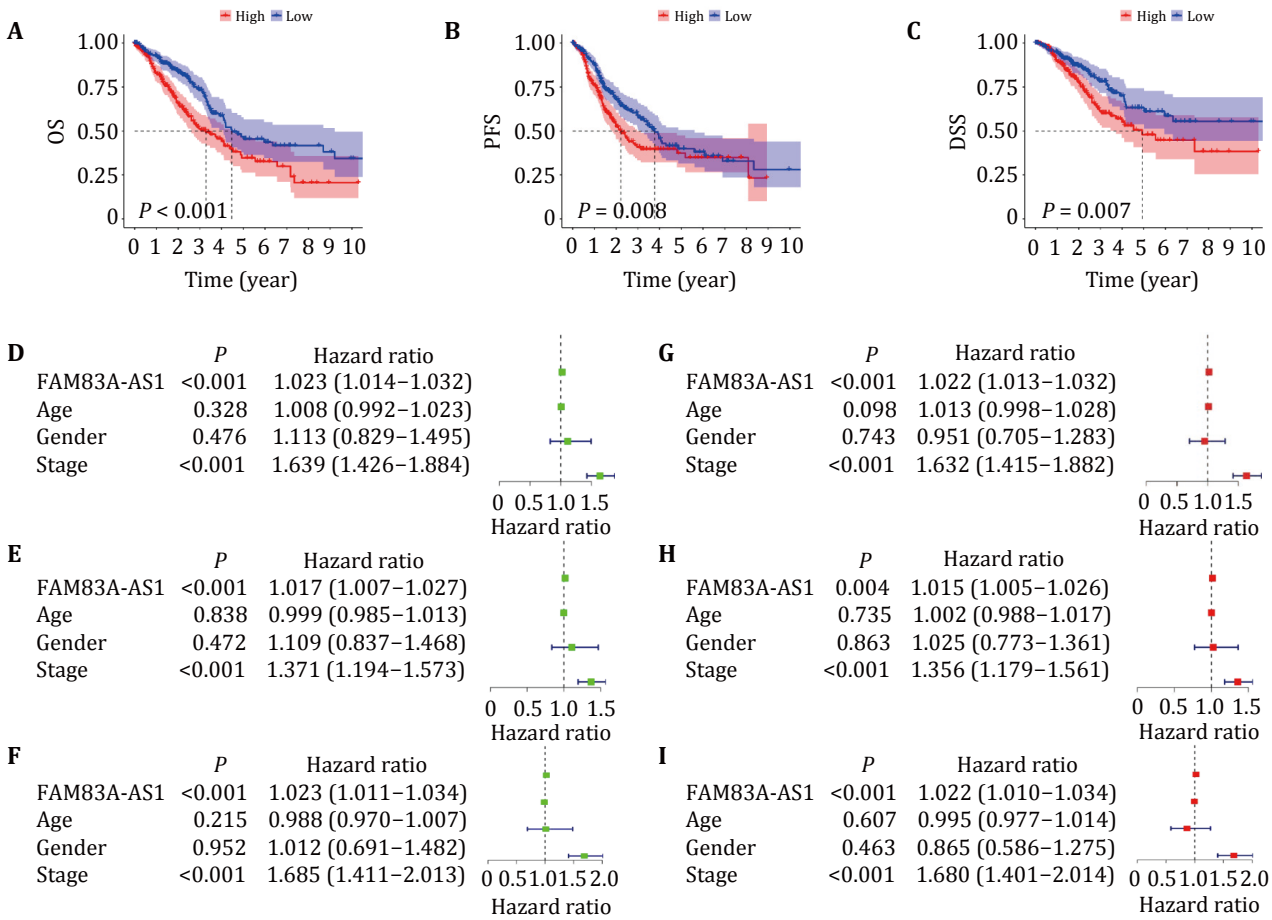

Fig. 3 K-M analysis and independent prognostic analysis of FAM83A-AS1. K-M analysis of FAM83A-AS1 for OS (**A**), PFS (**B**), and DSS (**C**). Univariate independent prognostic analysis of FAM83A-AS1 for OS (**D**), PFS (**E**), and DSS (**F**). Multivariate independent prognostic analysis of FAM83A-AS1 for OS (**G**), PFS (**H**), and DSS (**I**)

C5orf64 was higher, indicating that high expressions of LINC00535 and C5orf64 were associated with a higher survival rate (Figs. 6A and 6B). However, survival was significantly better in the low expression group than in the high expression group for the remaining four lncRNAs (CLDN10-AS1, LINC00518, THRB-IT1, and LNX1-AS2), suggesting that low expressions of CLDN10-AS1, LINC00518, THRB-IT1, and LNX1-AS2 were associated with higher survival (Figs. 6C–6F).

Based on DElncRNA-DEmiRNA and DEmiRNA-DEmRNA interaction pairs in the ceRNA networks, we identified the downstream miRNAs of six prognostic lncRNAs and the target genes of these miRNAs. There are 7 miRNAs and 71 mRNAs in the ceRNA network that satisfy the interaction relationship. Finally, the interactions between 6 lncRNAs, 7 miRNAs, and 71 mRNAs were integrated to obtain a prognostic ceRNA network (Fig. 6G).

Construction of the NETs-related prognostic ceRNA networks

Comparing 1380 NETs-related lncRNAs with six prognostic lncRNAs, and selecting the intersection lncRNAs existing in both sets, only lncRNA THRB-IT1 met the requirements. Based on the interaction pairs in the prognostic ceRNA networks, 1 miRNA and 12 mRNAs were extracted to satisfy the DElncRNA-DEmiRNA and DEmiRNA-DEmRNA interaction relationships in the prognostic ceRNA networks. Finally, after pairing each validated interaction, we assembled the NETs-related lncRNA regulated prognostic ceRNA networks (Fig. 6H).

Enrichment analysis

To explore the biological functions of genes within the NETs-related prognostic ceRNA networks, enrichment analysis was performed by using the Metascape

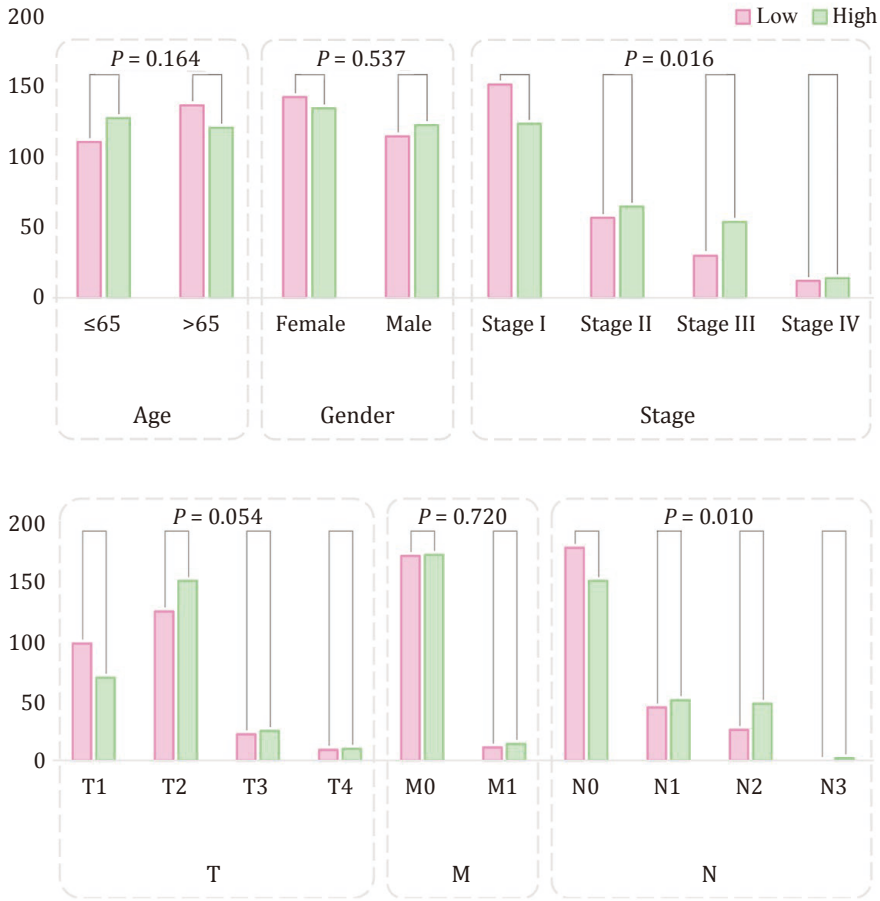

Fig. 4 Correlation analysis of FAM83A-AS1 expression and six clinical characteristics. The six clinical characteristics include: age, gender, pathologic stage, T, M, and N. The *P*-value indicates the statistical significance of differences between high and low expression groups within each clinical subgroup

database (https://metascape.org). The functional pathway enrichment analysis showed that the genes within the NETs-related prognostic ceRNA networks may be involved in biological processes such as nervous system development and cell junction organization (Fig. 7A). Furthermore, the disease-gene association enrichment analysis revealed that the genes within the NETs-related prognostic ceRNA networks were associated to varying degrees with multiple malignancies (Fig. 7B).

Regulatory relationship between NETs-related lncRNA TBX5-AS1 and promoter methylation site cg21907579

Differences in methylation sites and their distribution patterns

The differential analysis of methylation sites between normal and tumor samples identified 807 DMCs meeting the criteria of $P < 0.05$ and $|\log_2 FC| > 1$, comprising 740 hypermethylated sites and 67 hypomethylated sites. The promoter region of the gene is defined as the 1500 bp upstream and 500 bp downstream of the TSS. This region is divided into 40 bins, each spanning 50 bp. Then, 807 DMCs were mapped into 40 bins of the promoter region, and the average β values of hypermethylated and hypomethylated sites in 40 bins were calculated to evaluate the distribution pattern of DMCs in 40 bins of the promoter region. The average β value is calculated as follows:

$$\beta_i = \frac{\sum_{n=1}^{N} \beta_{i,n}}{N}, \quad (1)$$

$$\beta_{j,k} = \frac{\sum_{i=1}^{N_{j,k}} \beta_i}{N_{j,k}}, \quad (2)$$

$$\beta_j = \frac{\sum_{k=1}^{N_j} \beta_{j,k}}{N_j}, \quad (3)$$

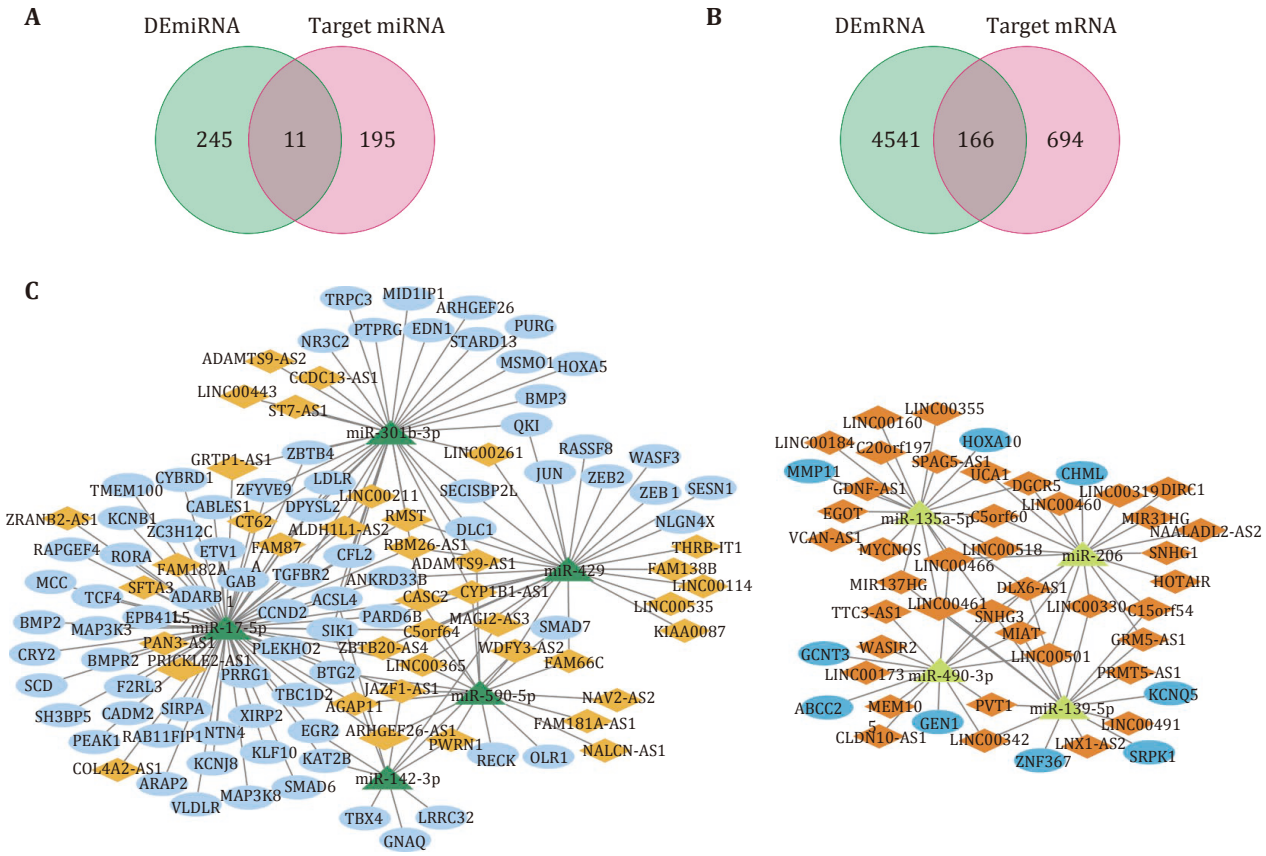

Fig. 5 Construction of ceRNA networks. **A** DEmiRNAs intersect with target miRNAs. **B** DEmRNAs intersect with target mRNAs. **C** A ceRNA network consisting of 79 lncRNAs, 9 miRNAs and 85 mRNAs was constructed. Diamonds represent lncRNAs, triangles represent miRNAs, ovals represent mRNAs, dark represents up-regulation, and light represents down-regulation

where n denotes the n-th sample, i denotes the i-th DMC, j denotes the j-th bin, and k denotes the k-th gene.

By computing the number of DMCs in each of the 40 bins, we found that hypermethylated sites outnumbered hypomethylated sites across the entire promoter. Notably, hypermethylated sites showed a pronounced enrichment near the TSS, with their gradually decreasing symmetrically toward both flanking regions (Fig. 8A). The average β values of hypermethylated and hypomethylated sites in 40 bins were calculated. The results showed that there were some differences in the distribution of average β values between hypermethylated and hypomethylated sites in 40 bins. Compared with the hypomethylated sites, the average β values of hypermethylated sites showed a relatively stable state near TSS, but the difference between the average β values of normal and tumor samples was generally consistent, ranging from 0.1 to 0.3 (Figs. 8B and 8C). After combining hypermethylated with hypomethylated sites, we observed that during LUAD development, hypermethylated sites with lower methylation levels in normal samples exhibited a trend toward increased methylation, while hypomethylated sites with higher methylation levels in normal samples showed a trend toward decreased methylation (Fig. 8D). Based on the distribution patterns of the number and β values of hypermethylated and hypomethylated sites, it is evident that hypermethylated sites significantly outnumber hypomethylated sites during LUAD development. This suggests that hypermethylated sites may play a more important role in the progression of LUAD.

DMCs regulate the expression of lncRNAs

Based on the annotation file, we selected lncRNAs and DMCs that map to the promoter regions of the corresponding lncRNAs. These lncRNAs are hereafter referred to as DMLs, yielding a total of 38 DMLs and 116 DMCs. Pearson correlation analysis between the 116 DMCs and their corresponding DMLs identified four DMC-DML pairs whose correlation coefficients met $|R| > 0.3$ and $P < 0.05$, and all four pairs exhibited a

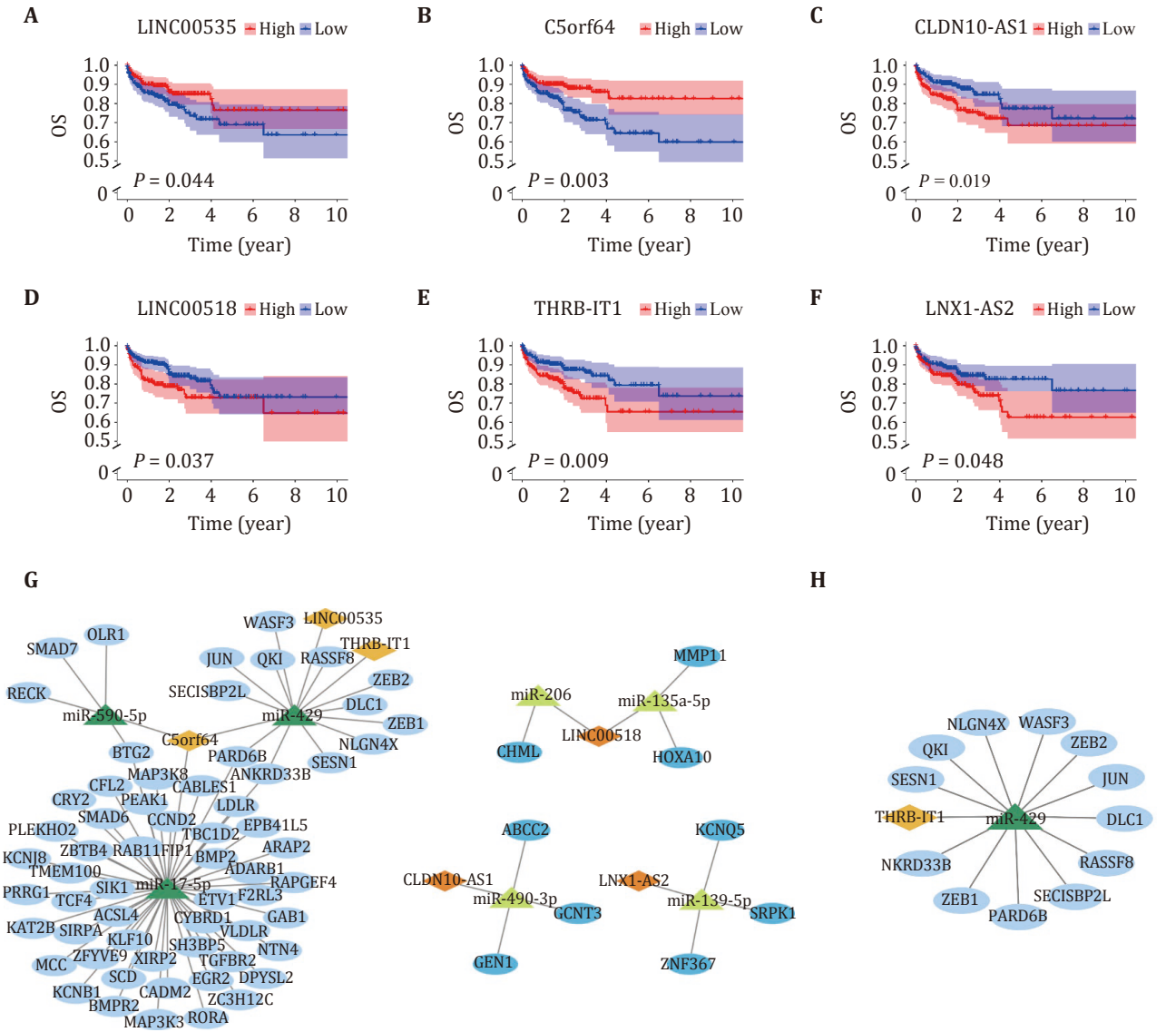

Fig. 6 Construction of NETs-related prognostic ceRNA networks. **A**–**F** K-M analysis of six prognostic lncRNAs. **G** A prognostic ceRNA network consisting of 6 lncRNAs, 7 miRNAs and 71 mRNAs was constructed. **H** A NETs-related prognostic ceRNA networks comprising 1 lncRNA, 1 miRNA, and 12 mRNAs

significant negative correlation (Figs. 9A–9D). Boxplots were plotted based on β values in the sample for the four DMCs, all of which exhibited partial methylation (Fig. 9E).

To obtain DMCs capable of modulating DMLs expression, a difference analysis was performed between DMCs and DMLs. The β values of four DMCs were different in normal form tumor samples, and four DMCs belonged to hypermethylation sites, while only three DMLs of the four DMLs had different expression between normal and tumor samples, and three DMLs belonged to down-regulated genes. Except for DML, whose expression did not change significantly, the remaining three pairs showed negative correlation between DMCs and DMLs, which was consistent with the above analysis results (Figs. 10A–10F).

DMC cg21907579 regulates the expression of NETs-related lncRNA TBX5-AS1

The intersection of the set containing 1380 NETs-related lncRNAs with the three DMLs yielded one pair of DMC-DML. The correlation between DML TBX5-AS1 and DMC cg21907579 was stronger than that between the other two pairs of DMC-DML, and three pairs of DMC-DML exhibited a negative correlation (Table 1).

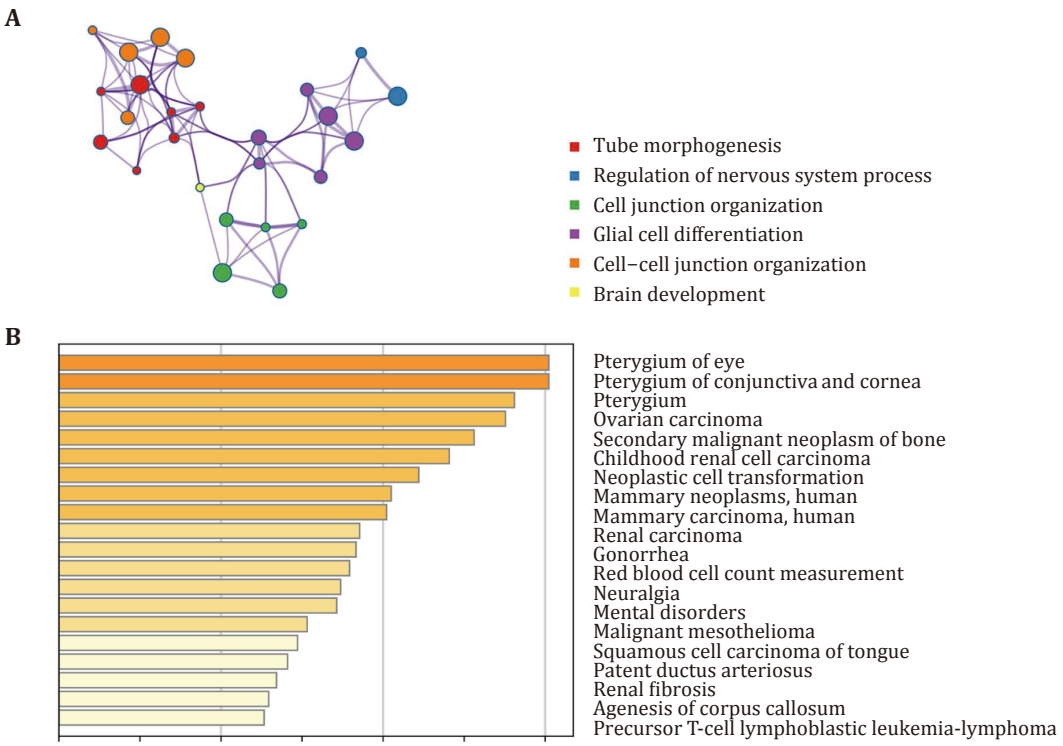

Fig. 7 The potential biological significance of genes within the NETs-related prognostic ceRNA networks. **A** Functional pathway enrichment analysis. **B** Disease-gene association enrichment analysis

Fig. 8 Distribution patterns of DMCs in promoter regions. **A** Number of DMCs across 40 bins. **B** Distribution of average β values for hypermethylated sites. **C** Distribution of average β values for hypomethylated sites. **D** Distribution of average β values for DMCs

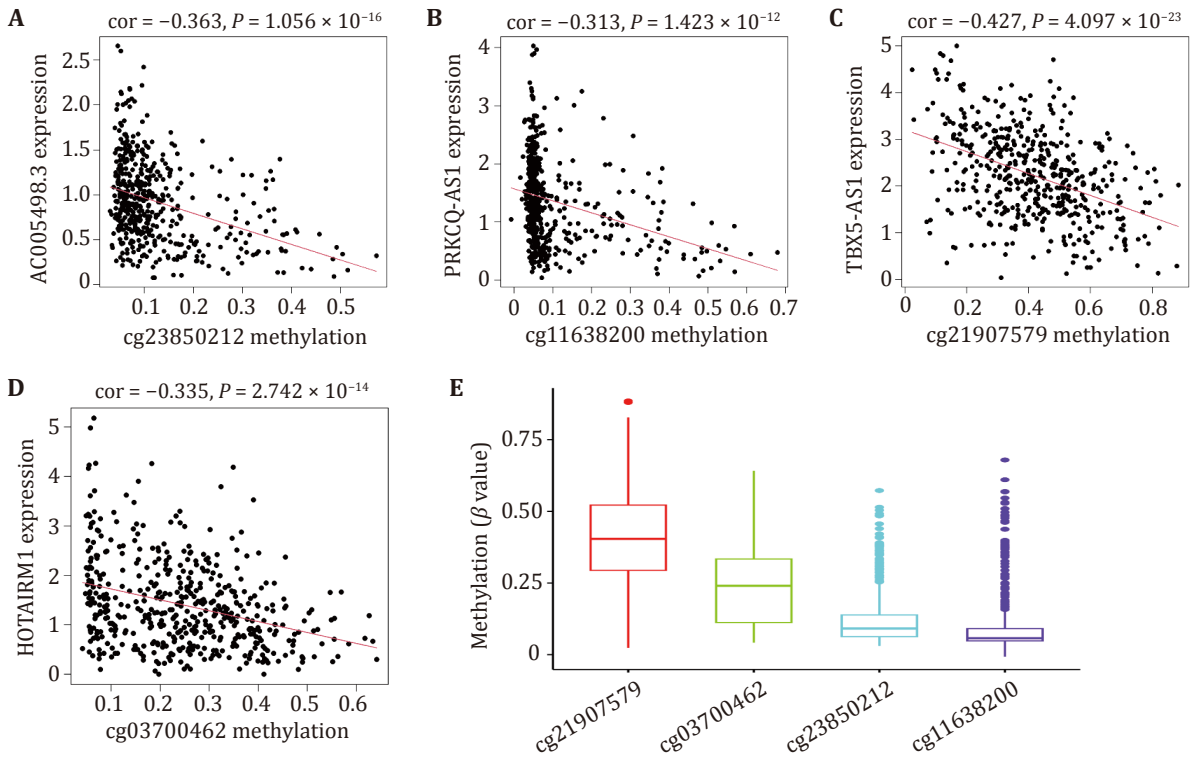

Fig. 9 Correlation analysis of four pairs of DMC-DML and the methylation degree of four DMCs. **A**–**D** Correlation analysis of four pairs of DMC-DML. **E** Degree of methylation of the four DMCs

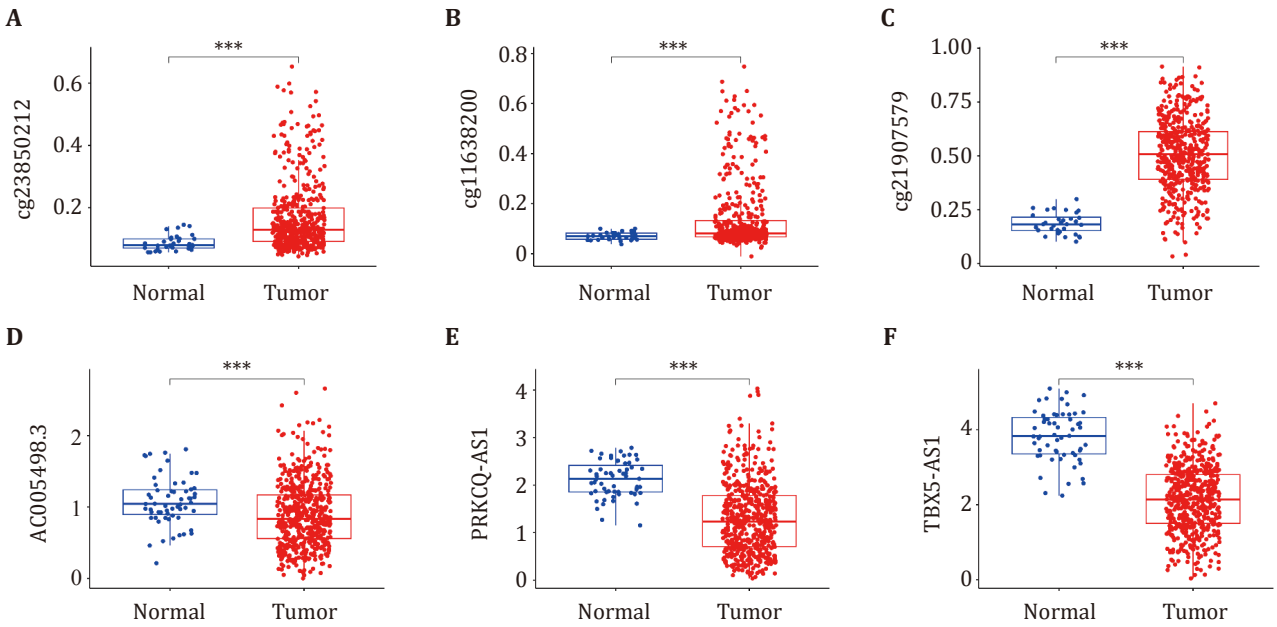

Fig. 10 Differential analysis of DMCs and DMLs. **A**–**C** Differential analysis of four DMCs between normal and tumor samples. **D**–**F** Differential analysis of four DMLs between normal and tumor samples

These results indicate that increased methylation at cg21907579 may down-regulate the NETs-related lncRNA TBX5-AS1, thereby potentially promoting LUAD progression.

Table 1 Correlation analysis of DMCs and DMLs

DMC/DML	*R*	Correlation
cg23850212 AC005498.3	−0.363	Negative
cg11638200 PRKCQ-AS1	−0.313	Negative
cg21907579 TBX5-AS1	−0.427	Negative

DISCUSSION

In this study, we employed bioinformatic approaches to identify three NETs-related lncRNAs (FAM83A-AS1, THRB-IT1, and TBX5-AS1) and systematically explored their potential significance in LUAD. The results indicate that FAM83A-AS1 can serve as an early diagnostic biomarker for LUAD patients, enabling the preliminary diagnosis of LUAD. At present, the carcinogenic effect of FAM83A-AS1 in LUAD has been confirmed by many studies. For example, FAM83A-AS1 is highly expressed in LUAD and is associated with poor prognosis in patients. FAM83A-AS1 promotes the proliferation and metastasis of LUAD by affecting the ERK signaling pathway and FAM83A expression (Wang *et al.* 2021). The elevated FAM83A-AS1 expression is closely associated with larger tumor size, lymph-node metastasis, and advanced T, N, and M in LUAD. Acting as a ceRNA, FAM83A-AS1 sequesters miR-150-5p, thereby relieving the repression of its target gene MMP14 and promoting LUAD cell proliferation, migration, invasion, and epithelial–mesenchymal transition *in vitro* (Xiao *et al.* 2019a).

Within the constructed ceRNA networks, THRB-IT1 modulates the expression of downstream genes by sponging miR-429, thereby participating in the development of LUAD. Although the role of THRB-IT1 in LUAD has not been previously reported, studies have demonstrated that miR-429 is associated with progression in LUAD and other pathological subtypes. For example, miR-429 is down-regulated in LUAD and regulates lncRNA MALAT1 expression by binding to the 3′ UTR of the MALAT1; it can be competitively sequestered by both MALAT1 and RhoA, thereby promoting LUAD cell proliferation and epithelial–mesenchymal transition (Xiao *et al.* 2019b). The expression of miR-429 in serum is reduced in non-small-cell carcinoma patients, and serum miR-429 is affected by the expression of miR-429 in tissues, while serum miR-429 is associated with poor prognosis in non-small-cell carcinoma patients and can serve as an independent prognostic factor (Zhu *et al.* 2014). In addition, the diseases interacting with miR-429 were investigated by using the MDPredict web server (http://lab.malab.cn/soft/MDPredict/). The results indicated that miR-429 potentially interacts with various human malignancies, including adenocarcinoma, non-small-cell lung cancer, breast cancer, gastric cancer, and renal cell carcinoma.

Moreover, when examining the relationship between NETs-related lncRNAs expression and methylation, we observed a significant negative correlation between TBX5-AS1 and cg21907579. Elevated methylation at cg21907579 is likely to reduce TBX5-AS1 expression, thereby influencing LUAD progression. TBX5-AS1 has been reported to be important in a variety of pathological types, including LUAD. For example, TBX5-AS1 was identified as an enhancer RNA in LUAD. TBX5-AS1 may exert its effects in tumors through signaling pathways such as PI3K/AKT and Ras. Pan-cancer validation also indicates that TBX5-AS1 correlates with survival rates in four tumor types: adrenal cortical carcinoma, LUAD, endometrial carcinoma, and lung squamous cell carcinoma (Cheng *et al.* 2021). TBX5-AS1 exhibits tissue- and gender-specific expression, correlating with poor prognosis in male patients with lung squamous cell carcinoma. Its expression increases following activation of the androgen signaling pathway, and male patients with lung squamous cell carcinoma exhibiting high TBX5-AS1 expression harbor a malignant immune microenvironment (Yan *et al.* 2021).

In this study, the NETs-related lncRNAs FAM83A-AS1, THRB-IT1, and TBX5-AS1 were identified as potential biomarkers and therapeutic targets in LUAD. Our results further reveal the molecular mechanism of NETs-related lncRNAs in the pathogenesis of LUAD, and provide potential diagnostic markers for LUAD patients and new insights into the treatment of LUAD patients.

MATERIALS AND METHODS

Data source

Gene expression and clinical data of LUAD patients were downloaded from the TCGA database (https://portal.gdc.cancer.gov/). Preliminary data cleaning was performed by using R to extract expression matrices for lncRNAs, miRNAs, mRNAs, and other clinical data matrices. The expression data matrix comprised 541

tumor samples and 59 normal samples. The clinical data matrix primarily included age, sex, pathologic stage, primary tumor (T), regional lymph node (N), and distant metastasis (M). T is used to assess the extent of local tumor growth. N is used to assess whether tumor cells have spread to nearby lymph nodes and the extent of such spread. M is used to assess whether tumor cells have spread to distant organs or tissues in the body. Stage denotes the overall classification of a tumor and is used to evaluate its developmental stage.

Methylation and survival data for LUAD were downloaded from the UCSC Xena database (https://xena.ucsc.edu/). The methylation sites within the 1500 bp upstream to 500 bp downstream regions of each transcription start site (TSS) were extracted by using Perl to filter the data. The methylation data matrix included 471 tumor samples and 32 normal samples. NETs-related genes were compiled from previously published studies (He *et al.* 2022; Jiang *et al.* 2023; Li *et al.* 2022; Quan and Huang 2022; Wu *et al.* 2022; Zhang *et al.* 2022; Zuo *et al.* 2023). After removing duplicates, 290 unique genes remained for the following analyses.

Difference analysis

The differential analyses of lncRNAs, miRNAs, mRNAs, and methylation sites between normal and tumor samples were performed by using the "limma" package in R. Features exhibiting significant differences were designated as differential lncRNAs (DElncRNAs), differential miRNAs (DEmiRNAs), differential mRNAs (DEmRNAs), and differentially methylated CpG sites (DMCs), respectively. DElncRNAs, DEmiRNAs, DEmRNAs, and DMCs were remained only if $FDR < 0.05$ and $|\log_2 FC| > 1$, where FDR represents the false rejection rate, also is known as the adjusted P value, representing the rejection rate of errors in multiple hypothesis tests, and FC represents the multiple difference, representing the degree of difference in gene expression between different biological samples.

Pearson correlation analysis

Pearson correlation analysis was used to calculate the correlation between DElncRNAs and NETs-related genes. The lncRNAs meeting the criteria of $|R| > 0.3$ and $P < 0.05$ were defined as NETs-related lncRNAs. Using the same criteria ($|R| > 0.3$, $P < 0.05$), we identified methylation sites whose methylation significantly correlated with lncRNAs expression, where R represents the Pearson correlation coefficient, representing the ratio of covariance to standard deviation of each of the two variables, calculated as follows:

$$R = \frac{\sum_{i=1}^{n}\left(X_i - \overline{X}\right)\left(Y_i - \overline{Y}\right)}{\sqrt{\sum_{i=1}^{n}\left(X_i - \overline{X}\right)^2}\sqrt{\sum_{i=1}^{n}\left(Y_i - \overline{Y}\right)^2}}, \quad (4)$$

where X_i represents the i-th sample value of variable X, and $\overline{X}$ represents the sample mean value of variable X. In addition, Pearson correlation analysis was performed on diagnostic lncRNA and six clinical characteristics, identifying clinical characteristics significantly associated with diagnostic lncRNA.

K-M analysis

The expression data were combined with survival data, and the samples were divided into high and low expression groups according to the expression amount of lncRNAs in DElncRNAs and ceRNA networks. K-M analysis was performed by using the "survival" package in R to obtain lncRNAs correlated with prognosis. In addition, K-M analyses of overall survival (OS), progression-free survival (PFS), and disease-specific survival (DSS) were performed on diagnostic lncRNA to verify the prognostic value of diagnostic lncRNA. In the K-M analysis, $P < 0.05$ indicates a statistically significant difference.

ROC curve

The ROC curves were used to evaluate a model's predictive performance through sensitivity and specificity, with the area under the ROC curve (AUC) closer to 1, representing higher predictive accuracy. The "timeROC" package in R was used to compute the AUC for each prognostic lncRNAs, calculated as follows:

$$AUC = \int_0^1 TPR d\left(FPR\right). \quad (5)$$

In discrete cases, AUC can be approximated by the trapezoidal rule, calculated as follows:

$$AUC = \sum_{i=1}^{n-1}\left(FPR_{i+1} - FPR_i\right)\frac{\left(TPR_{i+1} + TPR_i\right)}{2}. \quad (6)$$

FPR denotes for false positive rate, and TPR denotes for true positive rate. Finally, the results were visualized by using the "pROC" package in R. In general, $AUC = 1$ means that the model is a perfect classifier, $0.7 < AUC < 1$ indicates the model has good predictive performance, $0.5 < AUC < 0.7$ indicates that the model's predictive ability is only slightly better than random guessing, and $AUC = 0.5$ means the model's predictive capability is equivalent to random guessing.

Data availability statement

The related data for this paper is available in the TCGA database (https://portal.gdc.cancer.gov/) and UCSC Xena database (https://xena.ucsc.edu/).

Abbreviations

CeRNA	Competitive endogenous RNA
DElncRNA	Differentially expressed lncRNA
DEmiRNA	Differentially expressed miRNA
DEmRNA	Differentially expressed mRNA
DMC	Differentially methylated CpG site
DML	Differentially methylated CpG sites located at lncRNA
DSS	Disease-specific survival
LncRNA	Long non-coding RNA
LUAD	Lung adenocarcinoma
NETs	Neutrophil extracellular traps
OS	Overall survival
PFS	Progression-free survival

Acknowledgements This work was supported by the National Natural Science Foundation of China (62361047, 32160216).

Compliance with Ethical Standards

Conflict of interest Yuanyuan Zhao, Yingli Chen and Qianzhong Li declare that they have no conflict of interest.

Human and animal rights and informed consent This article does not contain any studies with human or animal subjects performed by any of the authors.

References

Chen P, Li Z, Hong Z, Zheng H, Zeng R (2023) Tumor type classification and candidate cancer-specific biomarkers discovery via semi-supervised learning. Biophys Rep 9(2): 57–66

Chen Q, Zhang L, Li X, Zhuo W (2021) Neutrophil extracellular traps in tumor metastasis: pathological functions and clinical applications. Cancers (Basel) 13(11): 2832. https://doi.org/10.3390/cancers13112832

Cheng L, Han T, Chen B, Nie K, Peng W (2021) TBX5-AS1, an enhancer RNA, is a potential novel prognostic biomarker for lung adenocarcinoma. BMC Cancer 21(1): 794. https://doi.org/10.1186/s12885-021-08517-w

Fang C, Liu F, Wang Y, Yuan S, Chen R, Qiu X, Qian X, Zhang X, Xiao Z, Wang Q, Fu B, Li Y (2021) A innovative prognostic symbol based on neutrophil extracellular traps (NETs)-related lncRNA signature in non-small-cell lung cancer. Aging (Albany NY) 13(13): 17864–17879

Gun SY, Lee SWL, Sieow JL, Wong SC (2019) Targeting immune cells for cancer therapy. Redox Biol 25: 101174. https://doi.org/10.1016/j.redox.2019.101174

He X, Xiao Y, Liu S, Deng R, Li Z, Zhu X (2022) Predicting the immune microenvironment and prognosis with a NETosis-related lncRNA signature in head and neck squamous cell carcinoma. Biomed Res Int 2022: 3191474. https://doi.org/10.1155/2022/3191474

Hidalgo A, Libby P, Soehnlein O, Aramburu IV, Papayannopoulos V, Silvestre-Roig C (2022) Neutrophil extracellular traps: from physiology to pathology. Cardiovasc Res 118(13): 2737–2753

Jiang T, Wang Y, Chen X, Xia W, Xue S, Gu L, Guo L, Lin H (2023) Neutrophil extracellular traps (NETs)-related lncRNAs signature for predicting prognosis and the immune microenvironment in breast cancer. Front Cell Dev Biol 11: 1117637. https://doi.org/10.3389/fcell.2023.1117637

Li Q, Chen W, Li Q, Mao J, Chen X (2022) A novel neutrophil extracellular trap signature to predict prognosis and immunotherapy response in head and neck squamous cell carcinoma. Front Immunol 13: 1019967. https://doi.org/10.3389/fimmu.2022.1019967

Liu S, Chen Y, Li Q, Fan Z, Li M, Du P (2024) A prognostic model for acute myeloid leukemia based on ferroptosis-related lncRNA and immune infiltration analysis. Biophys Rep 10(6): 377–387

Papayannopoulos V (2018) Neutrophil extracellular traps in immunity and disease. Nat Rev Immunol 18(2): 134–147

Qi Y, Song C, Zhang J, Guo C, Yuan C (2021) Oncogenic LncRNA CASC9 in cancer progression. Curr Pharm Des 27(4): 575–582

Quan J, Huang B (2022) Identification and validation of the molecular subtype and prognostic signature for clear cell renal cell carcinoma based on neutrophil extracellular traps. Front Cell Dev Biol 10: 1021690. https://doi.org/10.3389/fcell.2022.1021690

Sadeghi M, Dehnavi S, Jamialahmadi T, Johnston TP, Sahebkar A (2023) Neutrophil extracellular trap: A key player in the pathogenesis of autoimmune diseases. Int Immunopharmacol 116: 109843. https://doi.org/10.1016/j.intimp.2023.109843

Tan Y-T, Lin J-F, Li T, Li JJ, Xu R-H, Ju H-Q (2021) LncRNA-mediated posttranslational modifications and reprogramming of energy metabolism in cancer. Cancer Commun (Lond) 41(2): 109–120

Wang WY, Zhao Z, Xu C, Li C, Ding C, Chen J, Chen T, Zhao J (2021) LncRNA FAM83A-AS1 promotes lung adenocarcinoma progression by enhancing the pre-mRNA stability of FAM83A. Thorac Cancer 12(10): 1495–1502

Wang Y, Liu F, Chen L, Fang C, Li S, Yuan S, Qian X, Yin Y, Yu B, Fu B, Zhang X, Li Y (2022) Neutrophil extracellular traps (NETs) promote non-small cell lung cancer metastasis by suppressing lncRNA MIR503HG to activate the NF-κB/NLRP3 inflammasome pathway. Front Immunol 13: 867516. https://doi.org/10.3389/fimmu.2022.867516

Wei X, Li X, Hu S, Cheng J, Cai R (2023) Regulation of ferroptosis in lung adenocarcinoma. Int J Mol Sci 24(19): 14614. https://doi.org/10.3390/ijms241914614

Wu J, Zhang F, Zheng X, Zhang J, Cao P, Sun Z, Wang W (2022) Identification of renal ischemia reperfusion injury subtypes and predictive strategies for delayed graft function and graft survival based on neutrophil extracellular trap-related genes.

Front Immunol 13: 1047367. https://doi.org/10.3389/fimmu.2022.1047367

Xiao G, Wang P, Zheng X, Liu D, Sun X (2019a) FAM83A-AS1 promotes lung adenocarcinoma cell migration and invasion by targeting miR-150–5p and modifying MMP14. Cell Cycle 18(21): 2972–2985

Xiao H, Zhu Q, Zhou J (2019b) Long non-coding RNA MALAT1 interaction with miR-429 regulates the proliferation and EMT of lung adenocarcinoma cells through RhoA. Int J Clin Exp Pathol 12(2): 419–430

Yan T, Wang K, Zhao Q, Zhuang J, Shen H, Ma G, Cong L, Du J (2021) Gender specific eRNA TBX5-AS1 as the immunological biomarker for male patients with lung squamous cell carcinoma in pan-cancer screening. PeerJ 9: e12536. https://doi.org/10.7717/peerj.12536

Zhang Y, Guo L, Dai Q, Shang B, Xiao T, Di X, Zhang K, Feng L, Shou J, Wang Y (2022) A signature for pan-cancer prognosis based on neutrophil extracellular traps. J Immunother Cancer 10(6): e004210. https://doi.org/10.1136/jitc-2021-004210

Zhang Y (2024) LncRNA-encoded peptides in cancer. J Hematol Oncol 17(1): 66. https://doi.org/10.1186/s13045-024-01591-0

Zhou Q, Liu Y, Gao Y, Quan L, Wang L, Wang H (2024) Cuproptosis-related lncRNA predict prognosis and immune response of LUAD. Pharmgenomics Pers Med 17: 319–336

Zhu W, He J, Chen D, Zhang B, Xu L, Ma H, Liu X, Zhang Y, Le H (2014) Expression of miR-29c, miR-93, and miR-429 as potential biomarkers for detection of early stage non-small lung cancer. PLoS One 9(2): e87780. https://doi.org/10.1371/journal.pone.0087780

Zuo Y, Leng G, Leng P (2023) Identification and validation of molecular subtype and prognostic signature for lung adenocarcinoma based on neutrophil extracellular traps. Pathol Oncol Res 29: 1610899. https://doi.org/10.3389/pore.2023.1610899

